

# The Pattern of *p53* Mutations Caused by PAH *o*-Quinones is Driven by 8-oxo-dGuo Formation while the Spectrum of Mutations is Determined by Biological Selection for Dominance

Jong-Heum Park, Stacy Gelhaus, Srilakshmi Vedantam, Andrea L. Oliva, Abhita Batra, Ian A. Blair, Andrea B. Troxel,<sup>†</sup> Jeffrey Field, and Trevor M. Penning\*

*Department of Pharmacology, Centers for Excellence in Environmental Toxicology and Cancer Pharmacology, and Department of Biostatistics and Epidemiology, University of Pennsylvania School of Medicine, Philadelphia, Pennsylvania 19104-6084*

Received November 12, 2007

PAHs (polycyclic aromatic hydrocarbons) are suspect lung cancer carcinogens that must be metabolically converted into DNA-reactive metabolites. P4501A1/P4501B1 plus epoxide hydrolase activate PAH to ( $\pm$ )-anti-benzo[a]pyrene diol epoxide (( $\pm$ )-anti-BPDE), which causes bulky DNA adducts. Alternatively, aldo-keto reductases (AKRs) convert intermediate PAH *trans*-dihydrodiols to *o*-quinones, which cause DNA damage by generating reactive oxygen species (ROS). In lung cancer, the types or pattern of mutations in *p53* are predominantly G to T transversions. The locations of these mutations form a distinct spectrum characterized by single point mutations in a number of hotspots located in the DNA binding domain. One route to the G to T transversions is via oxidative DNA damage. An RP-HPLC-ECD assay was used to detect the formation of 8-oxo-dGuo in *p53* cDNA exposed to representative quinones, BP-7,8-dione, BA-3,4-dione, and DMBA-3,4-dione under redox cycling conditions. Concurrently, a yeast reporter system was used to detect mutations in the same cDNA samples. Nanomolar concentrations of PAH *o*-quinones generated 8-oxo-dGuo (detected by HPLC-ECD) in a concentration dependent manner that correlated in a linear fashion with mutagenic frequency. By contrast, micromolar concentrations of ( $\pm$ )-anti-BPDE generated (+)-*trans*-anti-BPDE-N<sup>2</sup>-dGuo adducts (detected by stable-isotope dilution LC/MS methodology) in *p53* cDNA that correlated in a linear fashion with mutagenic frequency, but no 8-oxo-dGuo was detected. Previous studies found that mutations observed with PAH *o*-quinones were predominately G to T transversions and those observed with ( $\pm$ )-anti-BPDE were predominately G to C transversions. However, mutations at guanine bases observed with either PAH-treatment occurred randomly throughout the DNA-binding domain of *p53*. Here, we find that when the mutants were screened for dominance, the dominant mutations clustered at or near hotspots primarily at the protein–DNA interface, whereas the recessive mutations are scattered throughout the DNA binding domain without resembling the spectra observed in cancer. These observations, if extended to mammalian cells, suggest that mutagenesis can drive the pattern of mutations but that biological selection for dominant mutations drives the spectrum of mutations observed in *p53* in lung cancer.

## Introduction

The *p53* tumor suppressor gene is mutated in a large portion of human cancer, including lung cancer. Studies of databases compiling *p53* mutations from over 20 000 tumor samples have identified three properties of the *p53* mutations in lung cancer (1–4). The first feature is a predominance of G to T transversions in *p53*. Other types of cancers show different mutational patterns, generally dominated by G to A transitions, suggesting that the carcinogens responsible for the mutations are different. This is the most unambiguous signature of lung cancer. The second property, called a strand bias, is that guanine bases are preferentially mutated in the nontranscribed strand suggesting that transcription-coupled repair occurs when the G lesion occurs on the transcribed strand. This causes a preponderance of G to T transversions relative to the complementary change of C to A. The third feature is mutation of a number of hotspot codons,

which account for about 50% of all the reported mutations. The most common hotspots are codons 248, 273, 249, 245, 158, and 157 but, with the exception of 157 and 158, most hotspot codons are also mutated in nonlung cancers. This suggests that, for the most part, the location of mutations is mutagen independent. Any molecular mechanism for lung-cancer initiation must account for these observations.

It is estimated that 85–90% of all lung cancer is observed in individuals that smoke (5). Tobacco smoke can cause oxidative stress and also contains a number of chemical carcinogens, including two major classes, the tobacco-specific nitrosamine 4-(methylnitrosamino)-1-(3-pyridyl)-1-butanone (NNK) and polycyclic aromatic hydrocarbons (PAH) (6). PAH are metabolically activated to either reactive diol-epoxides (7–10), (e.g., ( $\pm$ )-anti-BPDE)<sup>1</sup> by the combined action of P4501A1/1B1 and epoxide hydrolase or the intermediate *trans*-dihydrodiols are converted to reactive and redox-active PAH *o*-quinones by the action of aldo-keto reductases (AKR (1A1 and 1C1–1C4)) (11–15). In

\* To whom correspondence should be addressed. Tel: 215-898-9445. Fax: 215-573-2236. E-mail: penning@pharm.med.upenn.edu.

<sup>†</sup> Department of Biostatistics and Epidemiology, University of Pennsylvania School of Medicine.

<sup>1</sup> Abbreviations: ( $\pm$ )-anti-BPDE, anti-benzo[a]pyrene diol epoxide; BPQ, benzo[a]pyrene-7,8-dione; BAQ, benz[a]anthracene-3,4-dione; DMBAQ, dimethylbenz[a]anthracene-3,4-dione; PAH, polycyclic aromatic hydrocarbons.

previous studies, we examined the mutagenicity of ( $\pm$ )-*anti*-BPDE and PAH *o*-quinones using a yeast reporter gene assay that scored transcriptional competency of *p53* (16, 17). We reported that PAH *o*-quinones were highly mutagenic provided they were allowed to redox-cycle, and that the mutation pattern that dominated was G to T transversions. These mutations were abolished by reactive oxygen species (ROS) scavengers and, under the redox-cycling conditions employed, 8-oxo-dGuo could be detected by RP-HPLC-ECD in salmon testis DNA (18, 19). In the same assay, ( $\pm$ )-*anti*-BPDE was 80-fold less mutagenic than PAH *o*-quinones, and the mutation pattern observed was predominated by G to C transversions (17). Under these same reaction conditions, (+)-*trans-anti*-BPDE-N<sup>2</sup>-dGuo ((+)-*anti*-BPDE-N<sup>2</sup>-dGuo) bulky adducts could be detected in calf-thymus DNA using a stable-isotope dilution LC/MS assay (20). The detection of 8-oxo-dGuo adducts and (+)-*anti*-BPDE-N<sup>2</sup>-dGuo adducts in bulk DNA did not prove that these lesions could account for the mutations observed in *p53*. In our prior studies, adduct measurements in *p53* were not performed. Moreover, whereas PAH *o*-quinones yielded G to T transversions in *p53*, the mutations observed occurred randomly throughout the DNA-binding domain and did not recapitulate the mutational spectrum observed in lung cancer (16, 17, 21).

A “targeted mutagenesis” model has been proposed to account for the spectrum of mutations in lung cancer based on sequence specific DNA-adducts formed by ( $\pm$ )-*anti*-BPDE. In both treated cells and purified DNA, ( $\pm$ )-*anti*-BPDE will form adducts preferentially at many of the hotspots in *p53* including codons 157, 248, and 249 (22) in one study and codons 157, 248, and 273 in another study (23). Sequence specificity is enhanced by 5'-methylation of 5'-CpG-3' islands (24, 25). ( $\pm$ )-*Anti*-BPDE predominantly causes G to T transversions in most mutagenesis studies (21, 22, 26). Taken together, this suggests that ( $\pm$ )-*anti*-BPDE is an ultimate carcinogen by forming adducts at specific sites in *p53* to cause G to T transversions. However, the targeted mutagenesis model has been challenged by Rodin and Rodin who examined the *p53* database and failed to find significant differences in the spectrum of mutations between smokers and nonsmokers although they confirmed the predominance of G to T transversions in lung cancers (27, 28). They proposed that the lung cancer spectra of *p53* mutations resulted from biological selection and that smoke exposure enhanced the effects of an endogenous mutagen. Rodin and Rodin further speculated that reactive oxygen species (ROS), which have long been suspected as an ultimate carcinogen, may play the predominant role in lung carcinogenesis (27–29). In their model, ROS would cause the formation of 8-oxo-2'-deoxyguanosine (8-oxo-dGuo), leading to G to T transversions, whereas genetic selection for the most advantageous mutations would determine the spectrum. Tests of either hypothesis have been inconclusive because, although adducts can sometimes be observed in hotspot codons, mutagenesis experiments have not reproduced both the pattern of mutations (type of base changes) and spectrum of mutations (location of mutations by codon) observed in lung cancer.

To address these issues, we measured *p53* mutation with PAH *o*-quinones and ( $\pm$ )-*anti*-BPDE in the yeast reporter gene assay and used a portion of the same DNA for adduct analysis (8-oxo-dGuo and (+)-*anti*-BPDE-N<sup>2</sup>-dGuo). We found that in both instances a linear correlation existed between DNA-adducts and mutation frequency. To address the role of selection, we sorted PAH derived mutations into dominant and recessive mutants. With this filter in place, we showed that dominant mutations now cluster to hotspots observed in *p53* in lung cancer. Because G to T transversions are preferentially formed with PAH

*o*-quinones under redox-cycling conditions, we speculate that the mutation pattern observed in lung cancer may be attributed to 8-oxo-dGuo formation but that the mutational spectrum requires selection for dominance.

## Experimental Procedures

**Caution:** All PAHs are potentially hazardous and should be handled in accordance with the NIH Guidelines for the Laboratory Use of Chemical Carcinogens.

**Chemicals and Reagents.** BP-7,8-dione, BA-3,4-dione, and 7,12-DMBA-3,4-dione were synthesized according to published methods (30). ( $\pm$ )-*Anti*-BPDE was obtained from the National Cancer Institute, Chemical Carcinogen Standard Reference Repository (Midwest Research Institute, Kansas City, Missouri). All compounds were analyzed for purity and identity by LC/MS before use. YEASTMAKER Yeast Transformation and Plasmid Isolation Kit and all yeast culture media were purchased from Clontech (Palo Alto, CA). Adenine, L-leucine, L-tryptophan, DNase I (type II), alkaline phosphatase (type III from *Escherichia coli*), deferoxamine mesylate (desferal), and cupric chloride were purchased from Sigma-Aldrich Chemical Co. (St. Louis, MO). Phosphodiesterase I (PDE I, type II) from *Crotalus adamanteus* venom was acquired from Worthington Biochemical Corp. (Lakewood, NJ). Shrimp alkaline phosphatase (SAP) was acquired from Roche Diagnostics (Indianapolis, IN). 2'-Deoxyguanosine and [<sup>15</sup>N<sub>5</sub>]-dGuo were obtained from ICN Biomedical Inc. (Irvine, CA) and Spectra Stable Isotope (Columbia, MD), respectively. All other chemicals and enzymes were of the highest grade available, and all solvents for HPLC-ECD and LC-MS analysis were HPLC grade.

The ade reporter yeast strain, yIG397, and gap-repair expression vector pss16 were kindly provided by Dr. Richard Iggo (Swiss Institute for Experimental Cancer Research, 1066 Epalinges, Basel, Switzerland) (31, 32). Plasmid pTS76, which expresses wild-type *p53* using the TRP1 selectable marker, was a generous gift from Dr. Gilberto Fronza (33). Basic methods for yeast manipulations were carried out as described (34). Liquid media contained 0.67% yeast nitrogen base, 2% dextrose, 1% casamino acids, and 20  $\mu$ g/mL of adenine. Solid media for prototrophic selection of appropriate plasmids contained 0.67% yeast nitrogen base, 2% dextrose, and 2% agar with complete additions minus the relevant amino acids and nucleosides to select for auxotrophic markers.

**Yeast Assays.** Mutagenesis was performed using the *p53* cDNA fragment and pSS16 Gap-Repair vector as described previously (16). For the *p53* gap repair assay, 0.5  $\mu$ g of the mutagen-treated *p53* cDNA with carrier DNA was dissolved in 50  $\mu$ L of TE buffer (pH 8.0). Next, 15  $\mu$ L of the DNA sample (150 ng *p53* cDNA plus 100  $\mu$ g carrier DNA) was then mixed with 100 ng of the pSS16 gapped-vector and cotransformed into the yeast host strain yIG397 (grown to a OD<sub>600</sub> 0.6–0.9) using the lithium acetate procedure according to the YEASTMAKER™ Yeast transformation System Kit (CLONTECH). Yeast colonies expressing wild-type *p53* are white and yeast colonies expressing mutant *p53* are red. Red colonies were clearly identifiable after three days at 30 °C but the color is more intense after an additional 2 days at 4 °C. The spontaneous or background rate of mutation frequency in the assay was 0.4%. The mutation frequency was expressed as: [(number of red colonies – number of spontaneous red colonies)/total number of colonies] × 100 as previously described (16). The plasmids tested for dominance were described previously (17). To test dominance, we coexpressed wild-type *p53* from pTS76, a TRP1-derived plasmid (33), along with individual mutants (originally isolated as red colonies using a LEU2-based plasmid) and tested colonies on leu/trp plates. Recessive mutants become white, whereas dominant mutants become pink, although in most cases the colony was not as red as the original, and a range of color intensity was observed; all pink colonies were scored as dominant.

**PAH *o*-Quinone and ( $\pm$ )-*Anti*-BPDE Treatment.** The precipitated *p53* cDNA was recovered by centrifugation at 13 000 rpm for 30 min at 4 °C and rinsed with 70% ethanol. The pellet was dissolved in Chelex-treated 10 mM potassium phosphate buffer (pH

6.5), and the concentration of the hydrated DNA was measured using a Beckman DU640 UV/vis spectrophotometer. The DNA was divided into 4 and 24  $\mu\text{g}$  aliquots, respectively. A 4  $\mu\text{g}$  aliquot of the DNA was exposed to 125–700 nM of three PAH *o*-quinones (8% DMSO v/v), 180  $\mu\text{M}$  NADPH, and 100  $\mu\text{M}$  CuCl<sub>2</sub>, and a 24  $\mu\text{g}$  DNA aliquot was exposed to 0–20  $\mu\text{M}$  ( $\pm$ )-anti-BPDE (8% DMSO v/v) without NADPH and CuCl<sub>2</sub>. The samples were incubated for 3 h at 37 °C. After incubation, 0.5  $\mu\text{g}$  of DNA was taken from the sample and immediately mixed with 300  $\mu\text{g}$  of carrier DNA (herring testis) for the *p53* gap repair assay. Also, either 3.5  $\mu\text{g}$  of DNA was additionally saved from the PAH exposed samples for the analysis of 8-oxo-dGuo by RP-HPLC-ECD, or 20  $\mu\text{g}$  of DNA was saved for the analysis of (+)-anti-BPDE-N<sup>2</sup>-dGuo by stable isotope dilution LC/MS.

**Detection of 8-oxo-dGuo by HPLC-ECD.** To detect 8-oxo-dGuo in *p53* cDNA fragments, the quantitative digestion of *p53* cDNA was conducted as previously described, with minor modifications using precautions to prevent the adventitious oxidation of guanine (18, 19). The level of 8-oxo-dGuo was quantified by HPLC-ECD and expressed as 8-oxo-dGuo per 10<sup>5</sup> dGuo as previously described (18, 19).

**Detection of Stable (+)-Anti-BPDE-N<sup>2</sup>-dGuo Adducts by LC-MS.** To detect (+)-anti-BPDE-N<sup>2</sup>-dGuo adducts in the *p53* cDNA fragment, quantitative digestion of *p53* cDNA was conducted according to our previous protocol (16) with the following modification. The 20  $\mu\text{g}$  of ( $\pm$ )-anti-BPDE-treated *p53* cDNA pellet was dissolved in 300  $\mu\text{L}$  of 10 mM Tris-HCl (pH 7.4) containing 100 mM MgCl<sub>2</sub>. Ten microliters of DNase 1 (2 mg/3 mL 10 mM MOPS/100 mM MgCl<sub>2</sub> buffer) (Amersham Biosciences, Piscataway, NJ) was added and incubated for 1.5 h at 37 °C. Next, 150  $\mu\text{L}$  of 0.2 M glycine buffer (pH 10) was added along with 1 unit of PDE I, and the incubation was continued for 2 h at 37 °C. At the end of the incubation, 150  $\mu\text{L}$  of 50 mM Tris-HCl (pH 7.4) was added with 150  $\mu\text{L}$  of SAP 10X buffer and 30 units of SAP. The sample was incubated further for 2 h at 37 °C. An internal standard (12.5  $\mu\text{g}$ ) of (+)-trans-anti-BPDE-[<sup>15</sup>N<sub>5</sub>]-N<sup>2</sup>-dGuo was added to the digest. The *p53* cDNA digest was evaporated to dryness using a vacuum concentrator. The DNA was dissolved in 200  $\mu\text{L}$  of MeOH:H<sub>2</sub>O, 1:1 (v/v) and filtered through Costar Spin-X nylon centrifuge filter tube (Corning Incorporated, Corning, NY) before LC-MS and base analysis.

The anti-BPDE-N<sup>2</sup>-dGuo adducts in the DNA digest were measured by an Agilent 1100 HPLC system (Agilent Technology, Palo Alto, CA) equipped with a CTC autosampler (Leap Technology, Carrboro, NC) coupled to an MDS-Sciex API-4000 triple-quadrupole mass spectrometer (Applied Biosystems, Foster City, CA). The analysis of stable anti-BPDE-N<sup>2</sup>-dGuo adducts was conducted on a YMC J'sphere M80 Column (4  $\mu\text{m}$ ; 150 mm × 2.0 mm, 80 Å) using 5 mM NH<sub>4</sub>OAc with 0.02% formic acid as mobile phase A and methanol as mobile phase B at a flow of 200  $\mu\text{L}/\text{min}$ . The linear gradient started at 49% B and increased to 51% B in the first 20 min, followed by 51 to 65% B in 10 min, and continued to 100% B in 5 min. The mass spectrometer parameters were as follows: CID gas, 10 units; curtain gas, 30 units; ion source gas-1, 30 units; ion source gas-2, 10 units; ion spray voltage, 5.0 kV; ionization temperature, 500 °C; decluster potential, 50 V; entrance potential, 8 V; collision energy, 40 eV; collision cell exit potential, 22 V. MRM analyses were conducted in positive ESI mode using the following mass transitions: *m/z* 570.2(MH<sup>+</sup>, anti-BPDE-N<sup>2</sup>-dGuo) → *m/z* 257.1 (MH<sup>+</sup>-dGuo-H<sub>2</sub>O-CO); *m/z* 575.2 (MH<sup>+</sup>, anti-BPDE-[<sup>15</sup>N<sub>5</sub>]-N<sup>2</sup>-dGuo) → *m/z* 257.1 (MH<sup>+</sup>-[<sup>15</sup>N<sub>5</sub>]-dGuo-H<sub>2</sub>O-CO). The injection volume was 25  $\mu\text{L}$  for the samples. The anti-BPDE-N<sup>2</sup>-dGuo: anti-BPDE-[<sup>15</sup>N<sub>5</sub>]-N<sup>2</sup>-dGuo ratio was used to calculate adduct concentration based on interpolation of the calibration curve.

**Base Analysis and Anti-BPDE-N<sup>2</sup>-dGuo Adduct Quantitation.** DNA base analysis was conducted on a Hitachi Elite Chrom HPLC system (Hitachi High Technologies, San Jose, CA) equipped with a UV detector. The separation employed an XTerra MS5 C18 column (5  $\mu\text{m}$ ; 250 mm × 4.6 mm, 125 Å). As a mobile phase, Solvent A (5 mM NH<sub>4</sub>OAc, 0.02% formic acid) and solvent

B (100% methanol) was developed an XTerra MS5 C18 column (5  $\mu\text{m}$ ; 250 mm × 4.6 mm, 125 Å). The flow rate was set to 1 mL/min, and the nucleosides were eluted with 15% B. After 15 min, solvent B was increased to 100% for 5 min to wash off the column. This was followed by equilibration at initial conditions for another 5 min. The sample injection volume was 40  $\mu\text{L}$ , and DNA base levels were calculated by interpolation from the calibration curve. Overall adduct formation is given as a ratio of number of (+)-anti-BPDE-N<sup>2</sup>-dGuo adducts per 10<sup>5</sup> DNA bases.

**Statistical Analysis.** Data were analyzed by the Student's *t* test. Differences between treatment groups were considered significant at *p* < 0.05. All experiments were repeated at least 3 times. The data are presented as the mean ± SE values.

## Results

**PAH-DNA Modified Lesions Correlate with *p53* Mutagenesis.** Submicromolar concentrations of PAH *o*-quinones caused G to T transversions in *p53* cDNA but only when the *o*-quinones were allowed to redox cycle in the presence of NADPH and CuCl<sub>2</sub>. In the absence of redox-cycling, little to no mutagenesis was observed, and no mutations were observed when NADPH and CuCl<sub>2</sub> were tested alone (16, 17). The requirement for ROS and the predominance of G to T transversions suggest that the responsible lesion is 8-oxo-dGuo, a highly mutagenic modification that is often observed in smokers. Moreover, 8-oxo-dGuo is produced in salmon testis and calf thymus DNA by redox cycling *o*-quinones (18, 19). Because other oxidation products of guanine can occur, studies were also performed using the aldehydic reactive probe to detect aldehydic sites in bulk DNA following treatment with PAH *o*-quinones under redox cycling conditions. It was found that there was a linear correlation of aldehydic sites detected in the presence of 8-oxo-guanine glycosylase with 8-oxo-dGuo detected by HPLC-ECD. Furthermore, it was found that the rank order of oxidative lesions observed were 8-oxo-dGuo >> oxidized pyrimidines = abasic sites (19). To determine if 8-oxo-dGuo was responsible for *o*-quinone-induced mutations in *p53*, the *p53* gap repair assay was conducted using *p53* cDNA treated with *o*-quinones under redox-cycling conditions. Samples were divided and the treated DNA was analyzed both for 8-oxo-dGuo by RP-HPLC-ECD, and *p53* mutagenic frequency by the yeast *p53* gap repair assay. As a control, *p53* cDNA was treated with ( $\pm$ )-anti-BPDE and the sample analyzed for anti-BPDE-N<sup>2</sup>-dGuo adducts by stable isotope dilution LC/MS, 8-oxo-dGuo by RP-HPLC-ECD, and *p53* mutagenic frequency by the yeast *p53* gap repair assay.

We first measured the formation of 8-oxo-dGuo. Under redox-cycling conditions, a concentration-dependent formation of 8-oxo-dGuo in *p53* was observed with each of the PAH *o*-quinones tested. At 125–750 nM PAH *o*-quinone, the amount of 8-oxo-dGuo detected increased linearly to 150 ~ 600 adducts per 10<sup>5</sup> dGuo. The resultant rank order for 8-oxo-dGuo generation in *p53* cDNA was BA-3,4-dione > 7,12-DMBA-3,4-dione > BP-7,8-dione, in agreement with the previous data using salmon testis DNA (19), suggesting that the purified *p53* DNA was damaged by reactive oxygen. In contrast, no 8-oxo-dGuo was detected in *p53* when ( $\pm$ )-anti-BPDE was tested as the mutagen (part D of Figure 1). Stable isotope dilution LC-MS analysis revealed that stable (+)-anti-BPDE-N<sup>2</sup>-dGuo adducts were generated in the *p53* cDNA treated with ( $\pm$ )-anti-BPDE (Figure 2). Between 2.5  $\mu\text{M}$  and 20  $\mu\text{M}$ , the amounts of (+)-anti-BPDE-N<sup>2</sup>-dGuo adducts linearly increased to 150 ~ 940 adducts per 10<sup>5</sup> dGuo. We note that it required >20-fold more ( $\pm$ )-anti-BPDE than PAH *o*-quinone to achieve the same level of DNA adducts, consistent with previous mutagenesis data showing that >20-fold more ( $\pm$ )-anti-BPDE was required for mutagenesis (16, 17).

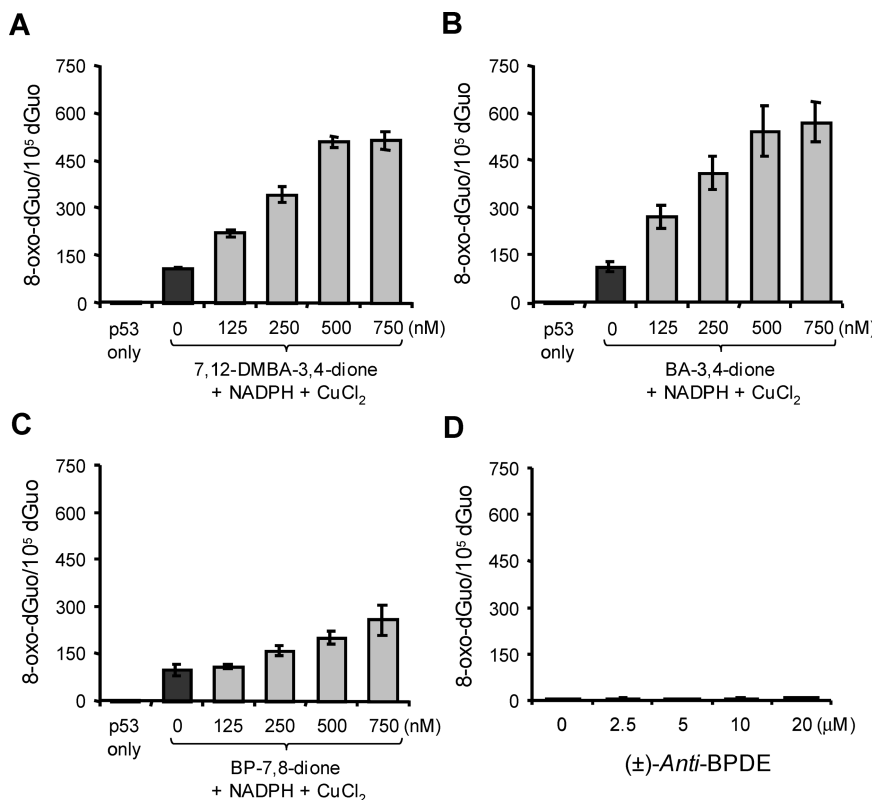


**Figure 1.** Formation of 8-oxo-dGuo in PAH treated *p53* DNA. In panels A, B, and C, *p53* cDNA was treated with increasing concentrations of PAH *o*-quinones under redox-cycling conditions, and 8-oxo-dGuo was measured as described in Materials and Methods. Panel D, ( $\pm$ )-*anti*-BPDE treated *p53* DNA.

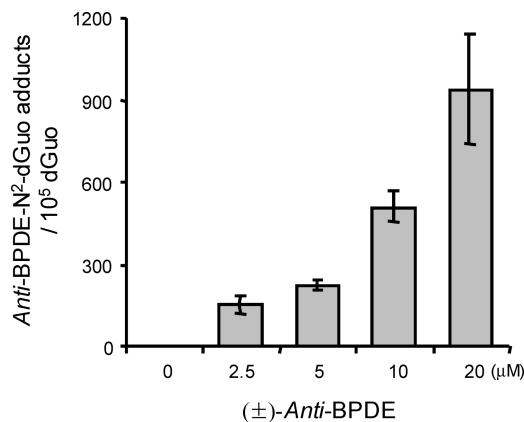


**Figure 2.** Formation of stable (+)-*anti*-BPDE-N<sup>2</sup>-dGuo adducts in ( $\pm$ )-*anti*-BPDE-treated *p53* cDNA. (+)-*anti*-BPDE-N<sup>2</sup>-dGuo adducts were measured in *p53* DNA treated with increasing concentrations of ( $\pm$ )-*anti*-BPDE as described in Materials and Methods.

We next compared the mutagenic frequency with the levels of DNA adducts (Figure 3). All three quinones showed a linear corelationship between 8-oxo-dGuo and mutagenic frequencies ( $R^2$  values for 7,12-DMBA-3,4-dione, BA-3,4-dione, and BP-7,8-dione were 0.896, 0.7896, and 0.825, respectively), suggesting that 8-oxo-dGuo was the mutagenic lesion responsible for the G to T transversions observed in PAH *o*-quinone-treated *p53*. On the other hand, the mutagenic effects of ( $\pm$ )-*anti*-BPDE on *p53* were not related to 8-oxo-dGuo formation but correlated with the formation of (+)-*anti*-BPDE-N<sup>2</sup>-dGuo adducts (Figure 4,  $R^2 = 0.8411$ ). This suggests that the mutagenic lesion caused by PAH *o*-quinones is 8-oxo-dGuo, whereas the mutagenic lesion caused by ( $\pm$ )-*anti*-BPDE is a stable bulky adduct. The slopes of each of these plots are quite comparable, suggesting

that the mutagenic potential of 8-oxo-dGuo and (+)-*anti*-BPDE-N<sup>2</sup>-dGuo were similar.

**The Spectrum of Dominant Mutations in Yeast Approximates the Tumor-Derived Spectrum.** Because many tumor-derived mutations, especially hotspot codons, are dominant negatives in transcriptional assays (33, 35, 36), we hypothesized that the spectrum of mutants from a randomly generated collection would more closely match the spectrum in tumors if only the dominant mutants were screened. To determine the spectrum of dominant mutations, we sorted *p53* mutations generated by *o*-quinones and ( $\pm$ )-*anti*-BPDE, previously reported and sequenced, into dominant and recessive mutants, and then plotted the spectra. The mutations generated by BA-3,4-dione and DMBA-3,4-dione were combined because they produce a common mutagen ROS. Not all of the mutations observed with BP-7,8-dione could be analyzed because of technical difficulties, but these showed the same trends observed with the other *o*-quinones. We also tested a set generated by ( $\pm$ )-*anti*-BPDE with methylated *p53* cDNA, because adducts have been reported to form more specifically at known hotspots in the methylated DNA (25). To test dominance, we coexpressed wild-type *p53* from a TRP1-selectable plasmid, along with individual mutants (originally isolated from a LEU2 selectable plasmid), and tested colonies on leu/trp plates. Recessive mutants become white, whereas dominant mutants become pink. In nearly all cases, the dominant mutants were not as red as the original colony, and a range of color intensity was observed as listed in Table 1. We found that 27 out of 129 plasmids with single point mutations were dominant (Table 1). The pattern of mutations in the dominant mutants was about the same as that when all mutants were scored and were dominated by G > T and C > A transversions in PAH *o*-quinone treated samples and G > C transversions in ( $\pm$ )-*anti*-BPDE treated samples. The most commonly mutated amino acid in the dominant

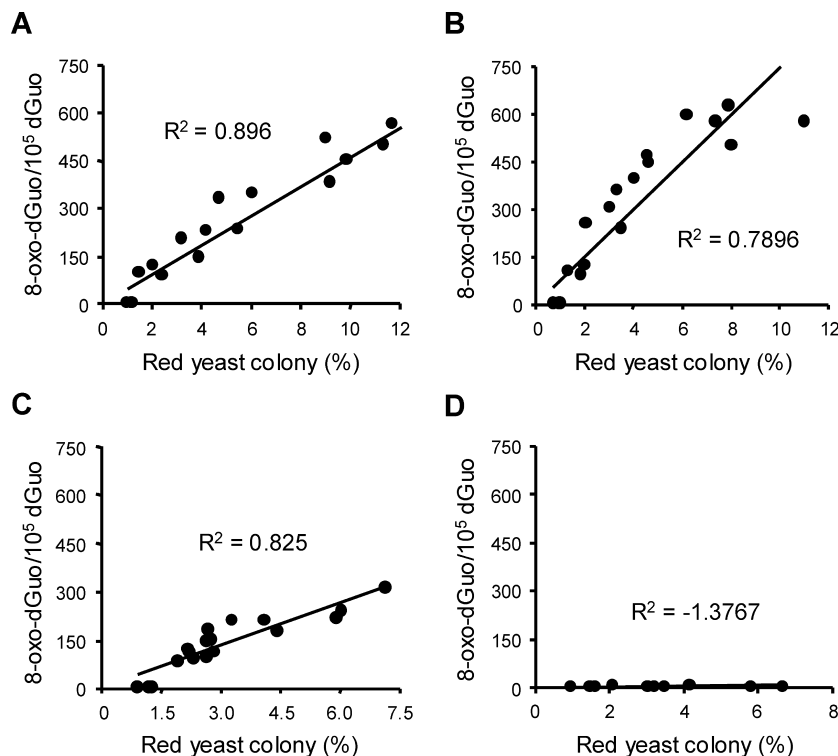


**Figure 3.** Relationship between 8-oxo-dGuo formation and mutation frequency of PAH *o*-quinone- and ( $\pm$ )-*anti*-BPDE-treated *p53* cDNA. Samples were treated with PAH metabolites, divided, and then analyzed for 8-oxo-dGuo or mutagenesis in the yeast assay as described in Materials and Methods. Data are plotted as 8-oxo-dGuo adduct formation vs % red yeast colonies. The treatments were (A) 7,12-DMBA-3,4-dione, (B) BA-3,4-dione, (C) BP-7,8-dione, and (D) ( $\pm$ )-*anti*-BPDE.

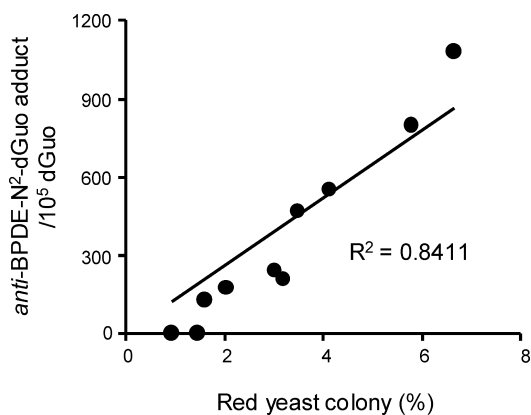


**Figure 4.** Relationship between stable (+)-*anti*-BPDE-N<sup>2</sup>-dGuo adduct formation and mutational frequency in ( $\pm$ )-*anti*-BPDE-treated *p53* cDNA. Samples were treated with ( $\pm$ )-*anti*-BPDE, divided, and then analyzed for (+)-*anti*-BPDE-N<sup>2</sup>-dGuo adducts or mutagenesis in the yeast assay as described in Materials and Methods. Data are plotted as (+)-*anti*-BPDE-N<sup>2</sup>-dGuo adduct formation vs % red yeast colonies.

mutants was arginine with 12 mutants (44%), which is also the most commonly mutated amino acid in the database (31%). (To reduce confusion over the mutations causing dominance, we plotted only those plasmids with single point mutations, although plasmids with multiple mutations are included in Table 1).

We defined hotspots as the codons that together account for 50% of the mutations in lung cancer based on the IARC database release R11 (this list differs from release R10 by the addition of codon 234 and is listed by the order of frequency in the legend to Table 2). Because the hotspots account for 24 of the 213 amino acids sequenced, a random distribution is 11.2%. Under all mutagenesis paradigms, the dominant mutations were enriched in hotspots. As shown in columns 4 and 2 of Table 2, 33% (9 of 27,  $P = 0.0002$ ) of the dominant mutants had single point mutations at hotspots mutated in lung cancer. If instead

we compared the dominant mutants against nonlung cancers, the incidence of hotspots was 44% (12 of 27) because hotspots (e.g., codon 213 is a nonlung cancer hotspot) vary slightly in the different tumors (Table 2). When analyzed by the PAH-treatment paradigm, 6 of the 16 dominant mutants (38%,  $P = 0.001$ ) from the PAH *o*-quinone treated samples were at hotspots. A similar trend was seen with ( $\pm$ )-*anti*-BPDE treated samples with 3 of 11 of the dominant mutants (27%) were at hotspots, but the numbers of mutants were too low to be significant ( $P = 0.062$ ). In our previous screens, we found that lung cancer hotspots are mutated about 20% of the time with *o*-quinones and 10% of the time with ( $\pm$ )-*anti*-BPDE, demonstrating that selection for dominance used in this study increases the percentage of mutations in hotspots (16, 17). As we define hotspots as the mutations that account for >50% of the mutations in tumors, our incidence of occurrence in the dominant mutants approaches that seen in the database. We believe that our data are underestimates because two plasmids with mutations in hotspot codon 248 were not included due to a second mutation. Additionally, the dominant mutations that were not located at hotspots were usually one or two residues away from a major hotspot, such as 244 and 279, which are near 245 and 280, respectively, suggesting they may interfere with DNA binding. Mutational spectra show that the majority of the dominant mutations, 88% (14 of the 16 isolated after PAH-*o*-quinone treatment), clustered in domains IV and V (Figure 5). The PAH *o*-quinone derived dominant mutations cluster near the protein-DNA interface and bear a striking resemblance to the cluster formed by the top 10 hotspots in lung cancer (parts A and B of Figure 6). The ( $\pm$ )-*anti*-BPDE derived dominant mutants did not cluster as strongly at the protein-DNA interface but did cluster in other hotspot regions, domain III, and codons 156–158, which lie between domains II and III. Thus, by

**Table 1. Dominant *p53* mutations arising from PAH metabolite treatment**

plasmid	treatment	codon	base change	AA change	dominance <sup>a</sup>	lung cancer hotspot <sup>b</sup>	nonlung cancer hotspot <sup>c</sup>	reported dominance <sup>d</sup>
BAQ15	BAQ	213	C > G	R > G	+++	N	Y	N
BAQ54	BAQ	213	C > T	R > STOP	+++	N	Y	N
BAQ22	BAQ	244	G > T	G > V	+	Y	Y	Y
BAQ32	BAQ	246	G > T	M > I	+	N	N	Y
BAQ18	BAQ	246	T > C	M > T	+	N	N	Y
BAQ4	BAQ	251	A > G	I > V	++	N	N	N/D
BAQ74	BAQ	256	A > C	T > P	+	N	N	N
BAQ59	BAQ	273	C > A	R > S	++	Y	Y	Y
BAQ1	BAQ	273	C > A	R > S	++	Y	Y	Y
BAQ75	BAQ	275	T > C	C > R	+	N	N	Y
DB3	DMBAQ	239	A > G	N > D	++	N	N	Y/N
DB13	DMBAQ	244	G > T	G > C	+	Y	Y	Y
DB2	DMBAQ	273	C > A	R > S	++	Y	Y	Y
DB30	DMBAQ	276	G > C	A > P	++	N	N	Y
DB48	DMBAQ	279	G > T	G > W	++	N	N	Y
DB62	DMBAQ	281	G > C	D > H	++	Y	N	Y
F22	BPDE	158	G > C	R > P	+	Y	Y	Y
F10	BPDE	176	G > C	C > S	+	Y	Y	Y
F4	BPDE	178	G > C	H > D	+	N	N	N
F11	BPDE	279	G > C	G > A	++	N	N	Y
F8	BPDE	283	G > C	R > P	++	N	N	Y/N
AM31	BPDE(me)	156	C > G	R > G	+	N	N	N/D
AM38	BPDE(me)	156	G > C	R > P	+	N	N	Y/D
AM41	BPDE(me)	158	C > G	R > G	+	Y	Y	Y
AM47	BPDE(me)	196	G > C	R > P	+	N	Y	N
AM23	BPDE(me)	213	C > T	R > STOP	++	N	Y	N
AM6	BPDE(me)	279	G > C	G > A	+++	N	N	Y
Plasmids with Multiple Mutations								
DB24	DMBAQ	248	G > T	R > L	++	Y	Y	Y
DB24	DMBAQ	278	C > A	P > H		N	Y	Y
DB31	DMBAQ	248	G > T	R > L	++	Y	Y	Y
DB31	DMBAQ	267	C > T	R > W		N	N	Y
F26	BPDE	156	G > C	R > P	+	N	N	Y/N
F26	BPDE	192	G > C	Q > H		N	N	N/D
AM7	BPDE(me)	131	C > T	N > N	+	N	N	N/D
AM7	BPDE(me)	257	T > A	L > Q		N	N	Y

<sup>a</sup> Mutants isolated after PAH metabolite treatments were tested for dominance (17). They are scored as +++, ++, or + based on the intensity of red color. The table also indicates if mutations are as listed below: <sup>b</sup> Lung cancer hotspots. <sup>c</sup> Nonlung cancer hotspots. <sup>d</sup> Previously reported as dominant in yeast (3). All dominant acting plasmids were resequenced; upon resequencing, plasmid DB31 was found to have an additional mutation at 267 and a clerical error confused plasmid AM31 with AM34. Corrected sequences are shown in the table. BPDE(me), *p53* cDNA was methylated prior to treatment with ( $\pm$ )-anti-BPDE. Unless indicated, plasmids were recessive.

**Table 2. Frequency of Mutations at Lung Cancer Hotspots Observed after Mutagen Treatment**

	total mutations	dominant mutations	recessive mutations	hotspots <sup>a</sup> dominant	hotspots recessive
DMBAQ	40	6	34	3 ( <i>P</i> = .003)	7
BAQ	37	10	27	3 ( <i>P</i> = .005)	3
<b>Quinone totals</b>	<b>77</b>	<b>16 (21%)</b>	<b>61 (79%)</b>	<b>6 (38%) (<i>P</i> = .001)</b>	<b>10 (16%)</b>
BPDE(methylated DNA)	32	6	26	1 ( <i>P</i> = .539)	4
BPDE	20	5	15	2 ( <i>P</i> = .043)	1
<b>BPDE totals</b>	<b>52</b>	<b>11 (21%)</b>	<b>41 (79%)</b>	<b>3 (27%) (<i>P</i> = .062)</b>	<b>5 (12%)</b>
<b>Grand totals</b>	<b>129</b>	<b>27 (21%)</b>	<b>102 (79%)</b>	<b>9 (33%) (<i>P</i> = .0002)</b>	<b>15 (15%)</b>

<sup>a</sup> Only plasmids with single point mutations are included. Hotspots are defined as the 24 mutations that account for 50% of the mutations reported in lung cancer in the IARC database release R11 (3). In order of frequency, these are codons: 248, 273, 249, 245, 158, 157, 175, 282, 179, 220, 242, 163, 176, 298, 154, 280, 266, 237, 281, 159, 173, 193, 234, and 244. The difference between this list and the previously used release R10 is the addition of codon 234. There are also minor differences in the rank order of the codons. P value calculations were performed to determine the significance that the hotspot frequencies observed differs from a random distribution of 11.3%, with 24 hotspots out of 213 amino acids sequenced. None of the frequencies of the hotspots for recessive mutations were significantly different than random (P values not shown). The table reports data from the PAH-quinones BAQ and DMBAQ; similar results were seen with BPQ (not shown).

combining mutagenesis with dominance selection, we found that the mutations clustered in all of the major hotspot regions.

In contrast to the clustering seen in the dominant mutations, only 15% of the recessive mutants (15 of 102) mapped to hotspots and were scattered throughout the DNA binding domain (Figure 5). Many mapped to the interdomain region between domains IV and V, which is rarely mutated in cancers and where no dominant mutations were found. There was a noticeable absence of recessive mutations in the DNA–protein interface (Figure 6). Several mutants were isolated multiple times, in which one plasmid was dominant while the other was recessive. We note that the plasmids were obtained through a random

mutagenesis and recombination paradigm, so they may contain additional mutations that could influence the dominance as well as the stability of the expressed *p53*. However, data suggest that while mutagenesis mechanisms determine the pattern of mutations, the spectrum of mutations is predominantly driven by biological selection.

## Discussion

This study provides additional support for *p53*-mutagenesis by PAH *o*-quinones mediated by reactive oxygen species and that aldo-keto reductases involved in their formation may

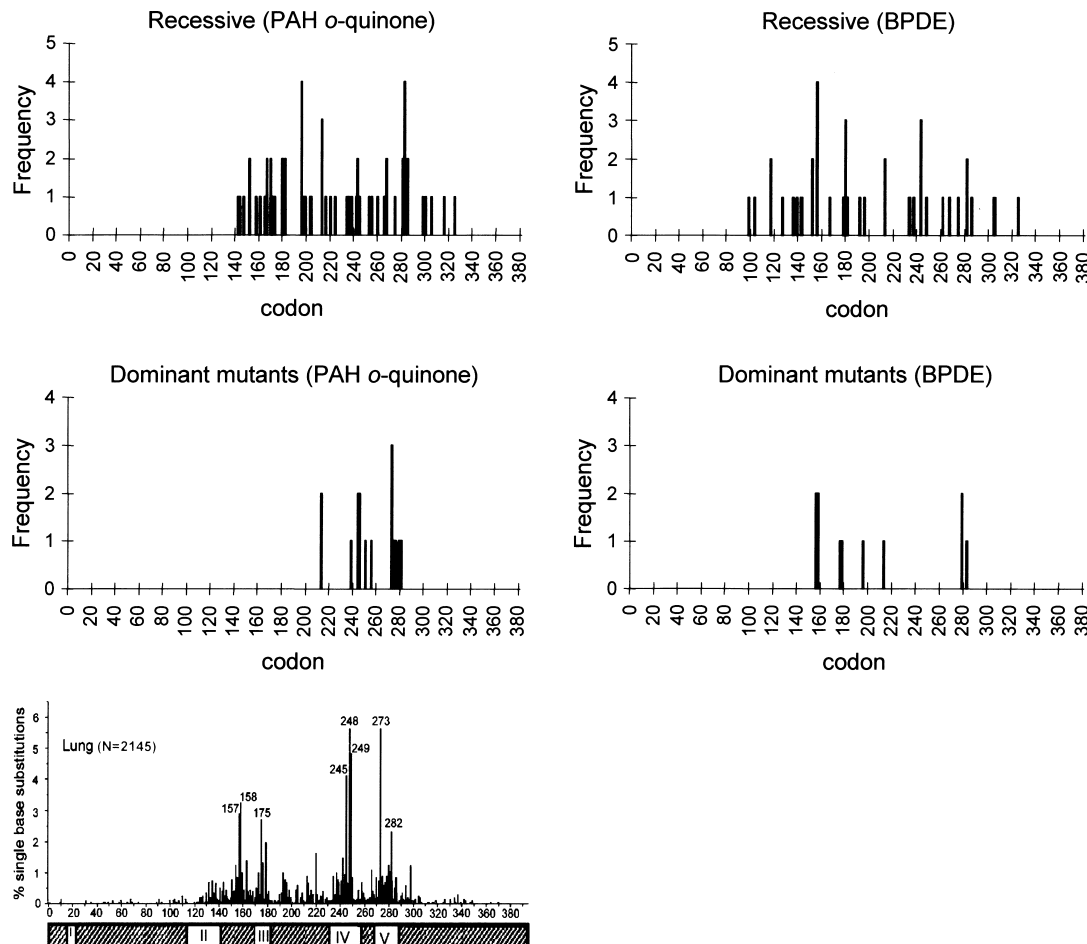


**Figure 5.** Spectra of dominant and recessive mutants observed in *p53* following PAH-treatment. The frequency of dominant and recessive mutations were plotted against codon number of *p53*. Data obtained from BAQ and DMBAQ were combined in the plots. The lower panel shows the spectrum of mutations in lung cancer distributed through its domain structure.

contribute to lung-cancer initiation. We find a linear correlation between the generation of 8-oxo-2'-deoxyguanosine and *p53*-mutagenesis. Whereas ROS can oxidize bases other than guanine, and other oxidation products of guanine are sometimes observed, 8-oxo-2'-deoxyguanosine has been studied most extensively because it is highly mutagenic and most prone to cause the G to T transversions characteristic of lung cancer (37, 38). 8-Oxo-2'-deoxyguanosine is also the most common lesion in PAH *o*-quinone treated DNA (19). As expected, we also observed a linear correlation between (+)-*anti*-BPDE-N<sup>2</sup>-dGuo and mutagenesis in ( $\pm$ )-*anti*-BPDE treated DNA but were unable to detect any 8-oxo-2'-deoxyguanosine. This correlation strongly implicates 8-oxo-2'-deoxyguanosine as the DNA adduct responsible for quinone induced *p53* mutagenesis. Additionally, we show for the first time in a mutagenesis assay, a close correlation of the tumor-derived spectrum by dominant but not by recessive or unselected mutants, suggesting that selection drives the tumor-derived spectrum.

Our *p53* mutagenesis assay allowed us to compare the potency of the different adducts by correlating levels of adducts with mutagenic frequency. We found that 8-oxo-dGuo and (+)-*anti*-BPDE-N<sup>2</sup>-dGuo adducts gave a similar mutagenic frequency based on adduct number. Thus, in our assays these two lesions are equipotent in producing mutations. However, the level of 8-oxo-dGuo adducts were achieved with >20-fold less PAH metabolite than required to produce the (+)-*anti*-BPDE-N<sup>2</sup>-dGuo lesions. We are unaware of a direct comparison of the mutagenic frequencies of these lesions previously.

The pattern of mutations observed in most studies with ( $\pm$ )-*anti*-BPDE are usually dominated by G > T transversions, which occur 70–80% of the time with most of the remainder being A > C transversions (26). One study found that ( $\pm$ )-*anti*-BPDE also caused G > T transversions in the same yeast assay that we use (21). However, other studies found a preference for G > C transversions in a yeast mutagenesis assay with ( $\pm$ )-*anti*-BPDE (39, 40). The preference for G to C over G to T transversions in yeast may be governed by the trans-lesional bypass polymerase Pol $\zeta$ , which has been shown to preferentially incorporate G opposite an (+)-*anti*-BPDE-N<sup>2</sup>-dGuo adduct in yeast strains proficient in mutagenesis (39, 40). Thus, while it was somewhat unexpected to observe fewer G > T mutations by ( $\pm$ )-*anti*-BPDE, we speculate that the repertoire of trans-lesion bypass polymerases that predominate in yeast differed from the studies of Yoon et al. Our observation that about 90% of the mutations seen with ( $\pm$ )-*anti*-BPDE were at GC base pairs is consistent with the formation of the (+)-*anti*-BPDE-N<sup>2</sup>-dGuo when we measured adduct formation.

**The Relationship between the Adduct Spectrum and the Mutagenic Spectrum.** The spectrum of *p53* mutations in lung and other cancers are characterized by a number of hotspots within the DNA-binding domain. Because several smoke-derived mutagens including ( $\pm$ )-*anti*-BPDE and acrolein (41) form adducts preferentially at guanine bases located in these hotspots, it has been argued that they preferentially target these sequences (23). Many of these sequences contain 5'CpG-3' islands and methylation of the 5'-cytosine may enhance

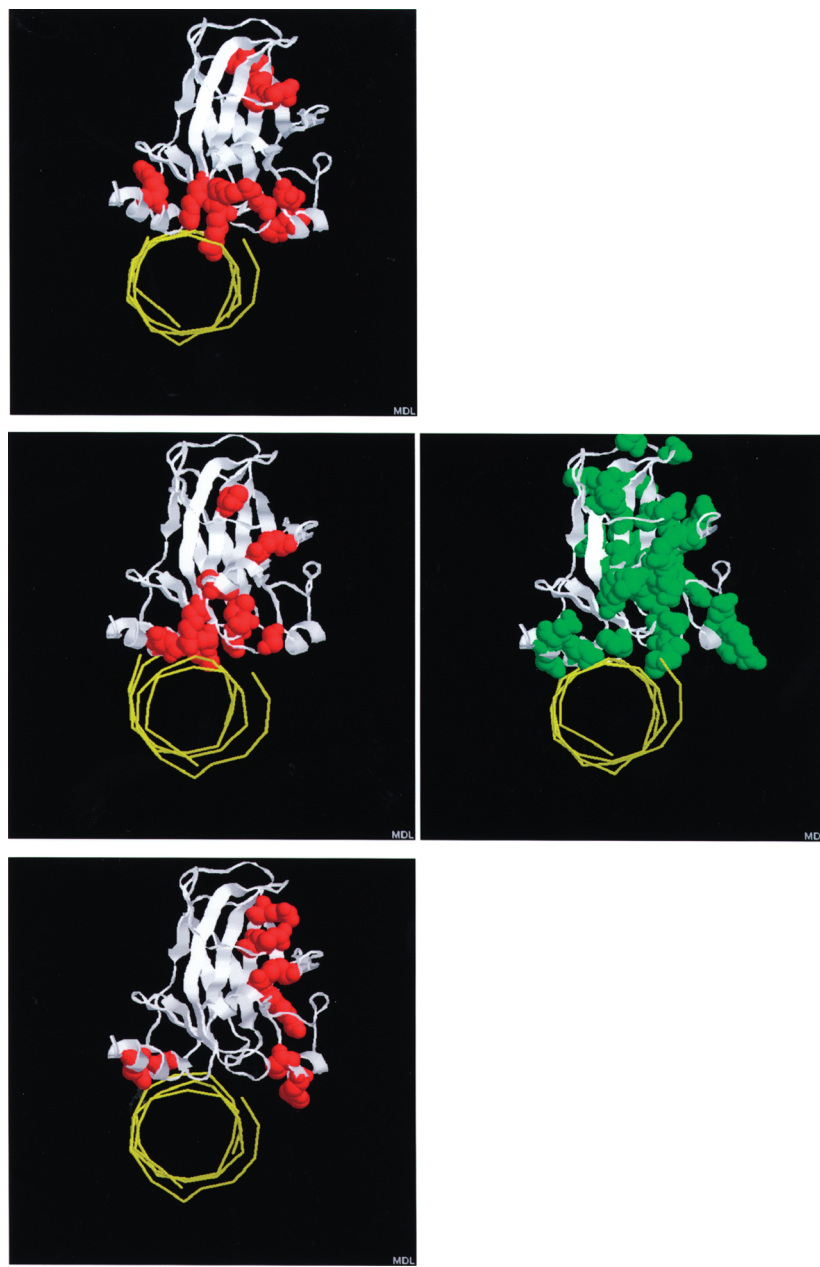


**Figure 6.** Mutations mapped onto the structure of *p53*. (A) The locations of the top 10 hotspots in lung cancer are shown in red. (B) The 11 unique PAH *o*-quinone derived dominant mutations from Table 1 are shown in red (213,239,244,246,251,256,273,275,276,279,281). The PAH *o*-quinone derived recessive mutations are shown in green (142,144,147,152,161,167,170,173,180,181,182,196,196,198,204,213,216,220,234,236,238,242,243,245,266,267,283,285,298,301,306,316,158,165,171,180,199,203,253,224,235,255,260,275,281,325). (C) The 8 unique BPDE derived dominant mutations are shown in red (156,158,176,178,196,213,279,283). Note that the dominant mutations cluster in DNA contact regions. Structures were plotted using the online software of the IARC TP53 database (3).

hydrophobic interaction and reactivity (24, 25). However, studies on targeting these sequences in *p53* did not measure adduct formation directly but instead located sites of adduction by ligation-mediated PCR.

In ligation-mediated PCR, the UvrABC endonuclease of the *E. coli* nucleotide excision repair pathway is used to cleave DNA on either side of a bulky DNA-adduct. After cleavage, a ligation-assisted PCR assay is used to amplify the DNA, and the products are run on sequencing gels to determine the site of adduction. If cleavage rates of adducted sequences differ based on sequence context, the assay may show codon bias. Alternatively, nonlinear amplification by PCR may amplify small differences in adduct formation at different codons. New direct methods to quantify (+)-*anti*-BPDE-N<sup>2</sup>-dGuo adducts at specific codons in *p53* have been developed using ds-oligonucleotides encoding exons 5, 7, and 8 site-specifically labeled with [<sup>15</sup>N]<sub>5</sub>-dGuo coupled with

MS. Although site-specific modification was observed at codons 156, 157, and 158 treated with ( $\pm$ )-*anti*-BPDE, the (+)-*anti*-BPDE-N<sup>2</sup>-dGuo adduct was predominately seen at codon 156, which is not a hot spot mutated in lung cancer (42, 43). Whereas these studies also found preference for adducts at codons 245, 248, and 273, more recent studies found that ROS could preferentially target codons 245 and 248, depending on the oxidant (44).

To date, ( $\pm$ )-*anti*-BPDE (23), acrolein (41), ROS (44), and even Chromium (45) have been shown to react preferentially with the same codons. Because the same codons react with so many mutagens, studies showing that a reactive intermediate forms adducts at specific codons do not conclusively incriminate that mutagen. We also find that when the mutational spectrum of the gene is considered rather than the adduct spectrum, little,

if any, specificity is observed in the spectra in the absence of biological selection.

**Selection versus Targeted Mutagenesis.** As an alternative to targeted mutagenesis, Rodin and Rodin have argued that genetic selection determines the *p53*-mutational spectrum in lung cancer (27, 28, 46). Several yeast mutational studies have generated patterns of mutations in *p53* dominated by lesions at guanines, but the mutations selected in yeast are scattered throughout the DNA binding region, showing no resemblance to the spectrum observed in tumors (16, 17, 21). Yet, when sorted into dominant and recessive mutations, we find a strong correlation between the tumor-derived spectrum and the dominant mutant spectrum. The similarity is perhaps most striking when considered by domain. We find that domains IV and V in particular stand out with clusters of dominant mutants in these two hotspot regions, whereas the interdomain region is a cold spot. These domains correspond to the surfaces of *p53* that contact DNA where most of the mutations in tumors are found (Figure 6). Our data strongly suggests that tumor-derived mutational spectra are predominantly driven by biological selection for the strongest, for example, dominant mutants. We note some exceptions to this conclusion.

**Dominant and Recessive Mutations in *p53*.** There are several observations that do not fit the simple conclusion that genetic dominance completely drives the spectrum. We, and others, have found that codon 279 is a strongly dominant mutant, and with its presence in four independent isolates, it was one of our most commonly isolated dominant mutations (33, 35). Yet in tumors, codon 279 is a cold spot and is rarely mutated. However, codon 279 is located in the DNA binding helix of domain V between the DNA contact residues 278 (a hotspot in all cancers but not lung cancer) and 280 (which is also a hotspot). We speculate that codon 279 mutations would provide a strong growth advantage to cells.

Of the dominant mutations isolated in this study, 19 have been previously reported as dominant, 4 have been reported as recessive (codons 213, 256, 178, 196), while no data are available on three (codons 156, 251, and 257) (3). Of the previously reported recessive mutants, we found that 256, 178, and 196 were weakly dominant, which may explain why they escaped detection. Codon 213, which was mutated in 3 plasmids that were strongly dominant, falls just outside of our definition of a lung cancer hotspot, ranking 25th, with 19 entries in the database. However, codon 213 is a hotspot in nonlung cancers and ranked 9th, with 320 entries. We found that half of the mutations in codon 213, even dominant plasmids, contained nonsense mutations that would truncate the protein. The dominance of some mutations in codon 213 may explain its relatively high frequency in the database.

By plotting the pooled recessive mutations, we also found a category of mutation, which we refer to as frequently isolated recessive mutations. We isolated multiple plasmids with mutations at codons 156, 196, 283, and 213 (213 was frequently found in both dominant and recessive plasmids; see above), qualifying them as recessive hotspots. All were also scored at least once as a dominant mutant. Interestingly, all four codons encode Arg residues and are located within CpG islands, which may be preferred sites of adduct addition. We speculate that these mutations cause strong loss-of-function mutants in *p53* and are readily isolated in yeast screens.

**Dominant Mutations and Tumorigenesis.** While generally regarded as a tumor suppressor, there are numerous properties of *p53* that suggest that dominance plays a central role in tumorigenesis. The spectrum of *p53* stands out from the spectra

of other tumor suppressors, such as NF1, NF2, and PTEN. The spectra of mutations in these tumor suppressors are characterized by clear loss-of-function mutations, whereas the *p53* spectrum is characterized by missense mutations. Mutant *p53* proteins are usually long-lived stable proteins, unlike wild-type *p53*, suggesting that the mutant proteins contribute to cell transformation. Some mutants even transform cells in cell transfection experiments. The case for dominance is also supported by numerous functional studies on mutants, showing that they are dominant in transcription assays, acting by forming nonfunctional tetramers with the wild-type *p53*. If dominance provides a growth advantage to the emerging tumor cell that is not provided by a recessive mutation, then the mutational spectrum would be enriched by dominant mutations. In fact, in some tumors dominant *p53* mutations correlate with early disease onset, but the relationship is not well established (47). Whereas we have focused our studies on selection for dominance, we note that there are other properties attributed to mutant *p53* proteins that may contribute to tumorigenesis, including cell transformation, NFKappaB activation, and stimulation of genetic instability (48, 49). These may account for some of the differences between our spectra of dominant mutations and the *p53* spectra seen in tumors.

**ROS and AKRs in Tobacco-Related Cancer.** Smokers have reduced levels of antioxidants, and excrete 8-oxo-2'-deoxyguanosine in their urine, suggesting that they are under oxidative stress. However, the measurements of 8-oxo-dGuo are often suspect due to problems of adventitious oxidation of guanine bases (50). Moreover, the detection of 8-oxo-dGuo in the urine suggests that this is repaired by nucleotide excision repair when base-excision repair normally repairs this lesion. Tobacco smoke can generate ROS through a number of compounds, including semiquinones (non-AKR derived), NO, and ozone (6, 29, 51). More recently, AKRs have emerged as an alternative pathway of tobacco-generated ROS. The ability of AKRs to form PAH *o*-quinones with the concomitant production of ROS is likely to occur in tobacco-related cancer because AKRs are consistently overexpressed in human lung adenocarcinoma (A549) cells, NSCLC, and SCLC, bronchial epithelial cells derived from NSCLC, or oral cancer cells (52–58). In addition, one allele of hOGG1 (8-oxo-guanine glycosylase, the base-excision repair enzyme responsible for the removal of 8-oxo-guanine) is absent in 50% of NSCLC patients suggesting that the reduced rates of repair of oxidatively damaged DNA may increase susceptibility to oxidative DNA damage (59, 60).

## Conclusions

In conclusion, we provide additional evidence for the AKR pathway of PAH *o*-quinone mutagenesis. We have implicated 8-oxo-dGuo as the most likely base lesion that causes the G to T transversions that predominate in *p53* mutational patterns. The spectrum of mutations is random under low-stringency selection, suggesting that adducts formed preferentially at specific codons are diluted out by nonbiased adducts when they proceed from a DNA lesion to a mutation. Instead, genetic selection, which we approximate by testing for dominance, is the predominant determinant of the spectrum.

We are left with one additional characteristic of the *p53* mutations observed in lung cancer that requires explanation, that is the strand bias for mutations on the nontranscribed strand. This could be explained by the loss of hOGG1 in lung cancer, which preferentially repairs the nontranscribed strand (61, 62). The strand bias can be examined in future studies involving the deletion of the yeast homologue of hOGG1 in our *p53* yeast reporter gene assay.

**Acknowledgment.** We thank Dr. Gilberto Fronza for the gift of plasmid pTS76. This work was supported by grants R01 CA39504 and P01 CA92537 awarded to T.M.P. and by grants R01 GM48241 and R01 ES015662, and pilot project support from 1P30 ES013508–01 to J.F. The contents of this publication are solely the responsibility of the authors and do not necessarily represent the official views of the NIEHS, NIH. We thank the NCI Chemical Carcinogen Standard Reference Repository for ( $\pm$ )-anti-BPDE.

## References

- Hollstein, M., Sidransky, D., Vogelstein, B., and Harris, C. C. (1991) *p53* mutations in human cancers. *Science* 253, 49–53.
- Beroud, C., and Soussi, T. (1998) *p53* gene mutation: Software and database. *Nucleic Acids Res.* 26, 200–204.
- Olivier, M., Eeles, R., Hollstein, M., Khan, M. A., Harris, C. C., and Hainaut, P. (2002) The IARC TP53 database: New online mutation analysis and recommendations to users. *Hum. Mutat.* 19, 607–614.
- Toyooka, S., Tsuda, T., and Gazdar, A. F. (2003) The TP53 gene, tobacco exposure, and lung cancer. *Hum. Mutat.* 21, 229–239.
- Edwards, B. K., Brown, M. L., Wingo, P. A., Howe, H. L., Ward, E., Ries, L. A., Schrag, D., Jamison, P. M., Jemal, A., Wu, X. C., Friedman, C., Harlan, L., Warren, J., Anderson, R. N., and Pickle, L. W. (2005) Annual report to the nation on the status of cancer, 1975–2002, featuring population-based trends in cancer treatment. *J. Natl. Cancer Inst.* 97, 1407–1427.
- Hecht, S. S. (1999) Tobacco smoke carcinogens and lung cancer. *J. Natl. Cancer Inst.* 91, 1194–1210.
- Jennette, K. W., Jeffery, A. M., Blobstein, S. H., Beland, F. A., Harvey, R. G., and Weinstein, I. B. (1977) Nucleoside adducts from the *in vitro* reaction of benzo[a]pyrene-7,8-dihydrodiol-9,10-oxide or benzo[a]pyrene-4,5 oxide with nucleic acids. *Biochemistry* 16, 932–938.
- Jeffrey, A. M., Jennette, K. W., Blobstein, S. H., Weinstein, I. B., Beland, F. A., Harvey, R. G., Kasai, H., Miura, I., and Nakanishi, K. (1976) Benzo[a]pyrene-nucleic acid derivative found *in vivo*: Structure of a benzo[a]pyrene-tetrahydrodiol epoxide-guanosine adduct. *J. Am. Chem. Soc.* 98, 5714–5715.
- Koreeda, M., Moore, P. D., Wislocki, P. G., Levin, W., Conney, A. H., Yagi, H., and Jerina, D. M. (1978) Binding of benzo[a]pyrene-7,8-diol-9,10-epoxides to DNA, RNA and protein of mouse skin occurs with high stereoselectivity. *Science* 199, 778–781.
- Osborne, M. R., Beland, F. A., Harvey, R. G., and Brookes, P. (1976) The reaction of ( $\pm$ )-7 $\alpha$ ,8 $\beta$ -dihydroxy-9 $\beta$ ,10 $\beta$ -epoxy-7,8,9,10-tetrahydrobenzo[a]pyrene with DNA. *Int. J. Cancer* 18, 362–368.
- Conney, A. H. (1982) Induction of microsomal enzymes by foreign chemicals and carcinogenesis by polycyclic aromatic hydrocarbons. G.H.A. Clowes Memorial Lecture. *Cancer Res.* 42, 4875–4917.
- Gelboin, H. V. (1980) Benzo[a]pyrene metabolism, activation and carcinogenesis: Role and regulation of mixed function oxidases and related enzymes. *Physiol. Rev.* 60, 1107–1166.
- Sutter, T. R., Tang, Y. M., Hayes, C. L., Wo, Y. -Y. P., Jabs, W., Li, X., Yin, H., Cody, C. W., and Greenlee, W. F. (1994) cDNA sequence of a human dioxin-inducible mRNA identifies a new gene subfamily of cytochrome P450 that maps to chromosome 2. *J. Biol. Chem.* 269, 13092–13099.
- Shimada, T., Hayes, C. L., Yamazaki, H., Amin, S., Hecht, S. S., Guengerich, F. P., and Sutter, T. R. (1996) Activation of chemically diverse procarcinogens by human cytochrome P450 1B1. *Cancer Res.* 56, 2979–2984.
- Penning, T. M., Burczynski, M. E., Hung, C.-F., McCoull, K. D., Palackal, N. T., and Tsuruda, L. S. (1999) Dihydrodiol dehydrogenases and polycyclic aromatic hydrocarbon activation: Generation of reactive and redox active *o*-quinones. *Chem. Res. Toxicol.* 12, 1–18.
- Yu, D., Berlin, J. A., Penning, T. M., and Field, J. (2002) Reactive oxygen species generated by PAH *o*-quinones cause change-in-function mutations in *p53*. *Chem. Res. Toxicol.* 15, 832–842.
- Shen, Y. M., Troxel, A. B., Vedantam, S., Penning, T. M., and Field, J. (2006) Comparison of *p53* mutations induced by PAH *o*-quinones with those caused by ( $\pm$ )-benzo[a]pyrene diol epoxide *in vitro*: Role of reactive oxygen and biological selection. *Chem. Res. Toxicol.* 19, 1441–1450.
- Park, J.-H., Gopishetty, S., Szewczuk, L. M., Troxel, A. B., Harvey, R. G., and Penning, T. M. (2005) Formation of 8-oxo-7,8-dihydro-2'-deoxyguanosine (8-oxo-dGuo) by PAH *o*-quinones: Involvement of reactive oxygen species and copper(II)/copper(I) redox cycling. *Chem. Res. Toxicol.* 18, 1026–1037.
- Park, J.-H., Troxel, A. B., Harvey, R. G., and Penning, T. M. (2006) Polycyclic aromatic hydrocarbon (PAH) *o*-quinones produced by the aldo-keto-reductases (AKRs) generate abasic sites, oxidized pyrimidines, and 8-oxo-dGuo via reactive oxygen species. *Chem. Res. Toxicol.* 19, 719–728.
- Ruan, Q., Kim, H. Y., Jiang, H., Penning, T. M., Harvey, R. G., and Blair, I. A. (2006) Quantification of benzo[a]pyrene diol epoxide DNA-adducts by stable isotope dilution liquid chromatography/tandem mass spectrometry. *Rapid Commun. Mass Spectrom.* 20, 1369–1380.
- Yoon, J. H., Lee, C. S., and Pfeifer, G. P. (2003) Simulated sunlight and benzo[a]pyrene diol epoxide induced mutagenesis in the human *p53* gene evaluated by the yeast functional assay: Lack of correspondence to tumor mutation spectra. *Carcinogenesis* 24, 113–119.
- Hussain, S. P., Amstad, P., Raja, K., Sawyer, M., Hofseth, L., Shields, P., Hewer, A., Phillips, D. H., Ryberg, D., Huagen, A., and Harris, C. C. (2001) Mutability of *p53* hotspot codons to benzo[a]pyrene diol epoxide (BPDE) and the frequency of *p53* mutations in nontumorous human lung. *Cancer Res.* 61, 6350–6355.
- Denissenko, M. F., Pao, A., Tang, M.-S., and Pfeifer, G. P. (1996) Preferential formation of Benzo[a]pyrene adducts at lung cancer mutation hotspots in P53. *Science* 274, 430–432.
- Denissenko, M. F., Chen, J. X., Tang, M. S., and Pfeifer, G. P. (1997) Cytosine methylation determines hot spots of DNA damage in the human P53 gene. *Proc. Natl. Acad. Sci. USA* 94, 3893–3898.
- Yoon, J. H., Smith, L. E., Feng, Z., Tang, M., Lee, C. S., and Pfeifer, G. P. (2001) Methylated CpG dinucleotides are the preferential targets for G-to-T transversion mutations induced by benzo[a]pyrene diol epoxide in mammalian cells: Similarities with the *p53* mutation spectrum in smoking-associated lung cancers. *Cancer Res.* 61, 7110–7117.
- Wei, S. J., Chang, R. L., Bhachech, N., Cui, X. X., Merkler, K. A., Wong, C. Q., Hennig, E., Yagi, H., Jerina, D. M., and Conney, A. H. (1993) Dose-dependent differences in the profile of mutations induced by (+)-7R,8S-dihydroxy-9S,10R-epoxy-7,8,9,10-tetrahydrobenzo(a)pyrene in the coding region of the hypoxanthine (guanine) phosphoribosyltransferase gene in Chinese hamster V-79 cells. *Cancer Res.* 53, 3294–3301.
- Rodin, S. N., and Rodin, A. S. (2000) Human lung cancer and *p53*: The interplay between mutagenesis and selection. *Proc. Natl. Acad. Sci. USA* 97, 12244–12249.
- Rodin, S. N., and Rodin, A. S. (2002) On the origin of *p53* G:C → T:A transversions in lung cancers. *Mutat. Res.* 508, 1–19.
- Ames, B., Gold, L., and Willett, W. (1995) The causes and prevention of cancer. *Proc. Natl. Acad. Sci. USA* 92, 5258–5265.
- Harvey, R. G., Dai, Q., Ran, C., and Penning, T. M. (2004) Synthesis of the *o*-quinones and other oxidized metabolites of polycyclic aromatic hydrocarbons implicated in carcinogenesis. *J. Org. Chem.* 69, 2024–2032.
- Ishioka, C., Frebourg, T., Yan, Y.-X., Vidal, M., Friend, S. H., Schmidt, S., and Iggo, R. (1993) Screening patients for heterozygous *p53* mutations using a functional assay in yeast. *Nat. Gen.* 5, 124–129.
- Flaman, J. M., Frebourg, T., Moreau, V., Charbonnier, F., Martin, C., Chappuis, P., Sappino, A. P., Limacher, J. M., Bron, L., Benhattar, J., Tada, M., Van Meir, E. G., Estreicher, A., and Iggo, R. D. (1995) A simple *p53* functional assay for screening cell lines, blood, and tumors. *Proc. Natl. Acad. Sci. USA* 92, 3963–3967.
- Monti, P., Campomenosi, P., Ciribilli, Y., Iannone, R., Inga, A., Abbondandolo, A., Resnick, M. A., and Fronza, G. (2002) Tumour *p53* mutations exhibit promoter selective dominance over wild type *p53*. *Oncogene* 21, 1641–1648.
- Guthrie, C., and Fink, G. R. (1991) *Guide to yeast genetics and molecular biology*. In Methods in Enzymology Academic Press: New York.
- Brachmann, R. K., Vidal, M., and Boeke, J. D. (1996) Dominant-negative *p53* mutations selected in yeast hit cancer hot spots. *Proc. Natl. Acad. Sci. USA* 93, 4091–4095.
- Dearth, L. R., Qian, H., Wang, T., Baroni, T. E., Zeng, J., Chen, S. W., Yi, S. Y., and Brachmann, R. K. (2006) Inactive full-length *p53* mutants lacking dominant wild-type *p53* inhibition highlight loss-of-heterozygosity as an important aspect of *p53* status in human cancers. *Carcinogenesis* 28, 289–298.
- Wang, D., Kreutzer, D. A., and Essigmann, J. M. (1998) Mutagenicity and repair of oxidative DNA damage: Insights from studies using defined lesions. *Mutat. Res.* 400, 99–115.
- Needle, W. L., and Essigmann, J. M. (2006) Mechanisms of formation, genotoxicity, and mutation of guanine oxidation products. *Chem. Res. Toxicol.* 19, 491–505.
- Xie, Z., Braithwaite, E., Guo, D., Zhao, B., Geacintov, N. E., and Wang, Z. (2003) Mutagenesis of benzo[a]pyrene diol-epoxide in yeast: requirement for DNA polymerase  $\zeta$  and involvement of DNA polymerase  $\eta$ . *Biochemistry* 42, 11253–11262.
- Zhao, B., Wang, J., Geacintov, N. E., and Wang, Z. (2006) Pol eta, Polzeta and Rev1 together are required for G to T transversion mutations induced by the (+)- and (-)-trans-anti-BPDE-N<sup>2</sup>-dG DNA adducts in yeast cells. *Nucleic Acids Res.* 34, 417–425.

- (41) Feng, Z., Hu, W., Hu, Y., and Tang, M. S. (2006) Acrolein is a major cigarette-related lung cancer agent: Preferential binding at *p53* mutational hotspots and inhibition of DNA repair. *Proc. Natl. Acad. Sci. USA* 103, 15404–15409.
- (42) Tretyakova, N., Matter, B., Jones, R., and Shallow, A. (2002) Formation of benzo[*a*]pyrene diol epoxide-DNA adducts at specific guanines within K-ras and *p53* gene sequences: Stable isotope-labeling mass spectrometry approach. *Biochemistry* 41, 9535–9544.
- (43) Matter, B., Wang, G., Jones, R., and Tretyakova, N. (2004) Formation of diastereomeric benzo[*a*]pyrene diol epoxide-guanine adducts in *p53* gene-derived DNA sequences. *Chem. Res. Toxicol.* 17, 731–741.
- (44) Tretyakova, N. (2006) Abstracts, American chemical society division of chemical toxicology, 232nd ACS national meeting, San Francisco CA, September 10–14, 2006. In: *Chem. Res. Toxicol.* 1698–1699.
- (45) Arakawa, H., Wu, F., Costa, M., Rom, W., and Tang, M. S. (2006) Sequence specificity of Cr(III)-DNA adduct formation in the *p53* gene: NGG sequences are preferential adduct-forming sites. *Carcinogenesis* 27, 639–645.
- (46) Rodin, S. N., and Rodin, A. S. (2005) Origins and selection of *p53* mutations in lung carcinogenesis. *Semin. Cancer Biol.* 15, 103–112.
- (47) Marutani, M., Tonoki, H., Tada, M., Takahashi, M., Kashiwazaki, H., Hida, Y., Hamada, J., Asaka, M., and Moriuchi, T. (1999) Dominant-negative mutations of the tumor suppressor *p53* relating to early onset of glioblastoma multiforme. *Cancer Res.* 59, 4765–4769.
- (48) Song, H., Hollstein, M., and Xu, Y. (2007) *p53* gain-of-function cancer mutants induce genetic instability by inactivating ATM. *Nat. Cell Biol.* 9, 573–580.
- (49) Kastan, M. B., and Berkovich, E. (2007) *p53*: a two-faced cancer gene. *Nat. Cell Biol.* 9, 489–491.
- (50) Gedik, C. M., and Collins, A. (2005) Establishing the background level of base oxidation in human lymphocyte DNA: Results of an interlaboratory validation study. *FASEB J.* 19, 82–84.
- (51) Murata, J.-I., Tada, M., Iggo, R. D., Sawamura, Y., Shinohe, Y., and Abe, H. (1997) Nitric oxide as a carcinogen: Analysis by yeast functional assay for inactivating *p53* mutations induced by nitric oxide. *Mutat. Res.* 379, 211–218.
- (52) Burczynski, M. E., Harvey, R. G., and Penning, T. M. (1998) Expression and characterization of four recombinant human dihydrodiol dehydrogenase isoforms: Oxidation of *trans*-7,8-dihydroxy-7,8-dihydrobenzo[*a*]pyrene to the activated *o*-quinone metabolite benzo[*a*]pyrene-7,8 dione. *Biochemistry* 37, 6781–6790.
- (53) Palackal, N. T., Burczynski, M. E., Harvey, R. G., and Penning, T. M. (2001) The ubiquitous aldehyde reductase (AKR1A1) oxidizes proximate carcinogen *trans*-dihydrodiols to *o*-quinones: Potential role in polycyclic aromatic hydrocarbon activation. *Biochemistry* 40, 10901–10910.
- (54) Hsu, N.-Y., Ho, H.-C., Chow, K.-C., Lin, T.-Y., Shih, C.-S., Wang, L.-S., and Tsai, C.-M. (2001) Overexpression of dihydrodiol dehydrogenase as a prognostic marker of non-small cell lung cancer. *Cancer Res.* 61, 2727–2731.
- (55) Fukumoto, S., Yamauchi, N., Moriguchi, H., Hippo, Y., Watanabe, A., Shibahara, J., Taniguchi, H., Ishikawa, S., Ito, H., Yamamoto, S., Iwanari, H., Hironaka, M., Ishikawa, Y., Niki, T., Sohara, Y., Kodama, T., Nishimura, M., Fukayama, M., Dosaka-Akita, H., and Aburatani, H. (2005) Overexpression of the aldo-keto reductase family protein AKR1B10 is highly correlated with smokers' non-small cell lung carcinomas. *Clin. Cancer Res.* 11, 1776–1785.
- (56) Penning, T. M. (2005) AKR1B10: A new diagnostic marker of non-small cell lung carcinoma in smokers. *Clin. Cancer Res.* 11, 1687–1690.
- (57) Woenckhaus, M., Klein-Hitpass, L., Grepmeier, U., Merk, J., Pfeifer, M., Wild, P., Bettstetter, M., Wuensch, P., Blaszyk, H., Hartmann, A., Hofstaedter, F., and Dietmaier, W. (2006) Smoking and cancer-related gene expression in bronchial epithelium and non-small-cell lung cancers. *J. Pathol.* 210, 192–204.
- (58) Nagaraj, N. S., Beckers, S., Mensah, J. K., Waigel, S., Vigneswaran, N., and Zacharias, W. (2006) Cigarette smoke condensate induces cytochromes P450 and aldo-keto reductases in oral cancer cells. *Toxicol. Lett.* 165, 182–194.
- (59) Lu, R., Nash, H. M., and Verdine, G. L. (1997) A mammalian DNA repair enzyme that excises oxidatively damaged guanines maps to a locus frequently lost in lung cancer. *Curr. Biol.* 7, 397–407.
- (60) Venkatesan, R. N., Bielas, J. H., and Loeb, L. A. (2006) Generation of mutator mutants during carcinogenesis. *DNA Repair* 5, 294–302.
- (61) Thomas, D., Scot, A. D., Barbey, R., Padula, M., and Boiteux, S. (1997) Inactivation of OGG1 increases the incidence of G.C. → T.A transversions in *Saccharomyces cerevisiae*: evidence for endogenous oxidative damage to DNA in eukaryotic cells. *Mol. Gen. Genet.* 254, 171–178.
- (62) Le Page, F., Klungland, A., Barnes, D. E., Sarasin, A., and Boiteux, S. (2000) Transcription coupled repair of 8-oxoguanine in murine cells: the ogg1 protein is required for repair in nontranscribed sequences but not in transcribed sequences. *Proc. Natl. Acad. Sci. USA* 97, 8397–8402.

TX700404A